Journal of Solid State Chemistry 183 (2010) 2925–2931

Contents lists available at ScienceDirect

Journal of Solid State Chemistry

journal homepage: www.elsevier.com/locate/jssc

Two new organic–inorganic hybrid compounds based on metal–pyrazine coordination polymers and Keggin polyoxometalates: effect of metal ions on the structure

Feng-Yun Cui, Xiao-Yu Ma, Cong Li, Tao Dong, Yuan-Zhe Gao, Zhan-Gang Han, Ying-Nan Chi *, Chang-Wen Hu *

Key Laboratory of Cluster Science, Ministry of Education of China, Beijing Institute of Technology, Beijing 100081, P.R. China

ARTICLE INFO

Article history:
Received 24 April 2010
Received in revised form
14 September 2010
Accepted 26 September 2010
Available online 1 October 2010

Keywords:
Keggin polyoxometalates
d^{10} Transition metal
Crystal structure
Electrocatalytic activities

ABSTRACT

Through changing the metal ions, two Keggin polyoxometalates-based hybrid compounds, $[Cu_5(pz)_6(Cl)(SiW_{12}O_{40})]$ (**1**) and $[Ag_4(pz)_3(H_2O)_2(SiW_{12}O_{40})]$ (**2**) (pz=pyrazine), were hydrothermally synthesized and characterized by an elemental analysis, IR spectroscopy, thermogravimetric analyses, and single X-ray diffraction. In compound **1**, the metal-organic motif exhibits a 6^3 topological 2-D sheet, which is further fused by the $[SiW_{12}O_{40}]^{4-}$ anions to construct a $(6\cdot7\cdot8)(6^3\cdot7\cdot8^2)(6^3)(6^5\cdot7)(6^5\cdot8)$ topological 3D structure. In compound **2**, the bridging groups $Ag_2(pz)$ connect the $[SiW_{12}O_{40}]^{4-}$ anions to form a $(5^3)_2(5^4\cdot8^2)$ topological 2-D layer, which is further linked by an $[Ag(pz)]_n^{n+}$ chains to construct a 3D structure with the $(3^4\cdot4^{16}\cdot5^{24}\cdot6^{12}\cdot7^8\cdot8^2)(3^4\cdot4^6\cdot5^4\cdot6)_2(4\cdot5^2)_2$ topology. It represents the highest connected network topology presently known for the polyoxometalates system. The structure differences of compounds **1** and **2** reveal that the coordination numbers and geometries of the metal ions have a great influence on the final structure and topology of the Keggin POMs-based hybrid compounds. In addition, the electrochemistry properties of the two compounds have been studied.

1. Introduction

The construction of metal-organic frameworks (MOFs) has been an area of rapid growth in recent years, because of their structure diversity and potential applications as functional materials [1–6]. Polyoxometalates (POMs), as early transition metal clusters, have many properties that make them attractive for applications in catalysis, biology, magnetism, optics, and medicine [7–13]. Hence, using the coordination ability of POMs to combine with different metal-organic units is a remarkable approach for constructing multifunctional materials [14–17]. This method may bring together the merits of each, such as structural diversity with unique framework topologies and the combination of the unique physical and chemistry properties of POMs with the feature of MOFs [18–20]. To date, numerous POMs-based coordination polymers with interesting structure and properties have been widely reported, in which POMs as template or inorganic building blocks induce the self-assembly of the MOFs [21–24]. However, the rational design and assembly of POMs-based coordination polymers still remain a long-term challenge. To achieve this aim, several factors must be taken into account, such as the coordination geometry of metal ions [25–29], the nature of organic ligands [30–33], the use of a variety of POMs [34–36], the pH of the reaction system [37–39] and the topological and geometrical relations between the metal ions and the ligand [40,41]. For example, Long's group has discussed the influences of steric hindrance of the organic ligands, the POM anions, and the pH values on the structure of POM-based hybrids [42–44]; Su's group has discussed the influence of metal ions on the structure of POMs-based hybrids [29]. However, studies of the influence of the factors on the structure of POMs-based hybrid are still rare and it would take more examples to rationalize the results.

With the hope of obtaining an informative example for designable syntheses, we chose Keggin polyanion, copper(I) and silver(I) ions, and ligand pyrazine (pz) to investigate the effect of the metal ions on the resultant structures of POMs-based coordination polymers. The following points are taken into consideration: (i) Keggin polyanions, as the most studied POMs types, have widely regarded as important molecular building units, because they have a large number of terminal and bridging oxygen atoms that are potential coordination sites; (ii) the d^{10} ions, as soft Lewis acidic metal ions, generally show variable coordination numbers and tunable coordination spheres; (iii) pyrazine, as a bridging bidentate ligand, commonly exhibits simple and controllable coordination mode and possesses small steric hindrance.

* Corresponding authors. Fax: +86 10 68912631.
E-mail address: cwhu@bit.edu.cn (C.-W. Hu).

0022-4596/$ - see front matter © 2010 Elsevier Inc. All rights reserved.
doi:10.1016/j.jssc.2010.09.034

Herein, two Keggin POMs-based hybrid, namely $[Cu_5(pz)_6(Cl)(SiW_{12}O_{40})]$ (**1**), $[Ag_4(pz)_3(H_2O)_2(SiW_{12}O_{40})]$ (**2**) have been synthesized by changing metal ions under hydrothermal conditions and characterized by the single-crystal X-ray diffraction. The influences of metal ions on the ultimate framework will be presented and discussed.

2. Experimental

2.1. Materials and general procedures

All reagents and solvents were purchased from commercial sources and used without further purification. IR spectra were obtained (as KBr pressed pellets) using a Nicolet 170SXFT/IR spectrometer. The X-ray powder diffraction (XPRD) of samples was collected on a Japan Rigaku D/max γ A X-ray diffractometer equipped with graphite-monochromatized Cu $K\alpha$ radiation (γ=0.154060 nm). The C, H, and N elemental analyses were performed on Perkin-Elmer 2400 CHN elemental analyzer. Inductively coupled plasma (ICP) spectra were performed on a Perkin-Elmer Optima 2000 ICP-OES spectrometer. X-ray photo-electron spectrometry (XPS) spectra were measured on a VG ESCALAB spectrometer. TG analyses were carried out in nitrogen atmosphere between 40 and 800 °C at a heating rate of 10 °C/min on a 2960 SDT simultaneous thermal analyzer. A CHI 440 electrochemical workstation connected to a Digital-586 personal computer was used for control of the electrochemical measurements and for data collection. Platinum gauze was used as a counter electrode and an Ag/AgCl electrode was referenced. Chemically bulk-modified carbon paste electrodes (CPEs) were used as working electrodes.

2.2. Syntheses

2.2.1. $[Cu_5(pz)_6(Cl)(SiW_{12}O_{40})]$ (**1**)

A mixture of $H_4SiW_{12}O_{40}$ (288 mg, 0.1 mmol), pz (13 mg, 0.1 mmol), $Cu(CH_3COO)_2\cdot 3H_2O$ (40 mg, 0.2 mmol) were dissolved in 8 ml of distilled water and stirred at room temperature for 30 min. When the pH value of the mixture was adjusted to 2–3 with 1 mol L^{-1} HCl, the cloudy solution was transferred and sealed in a 15-ml Teflon-lined stainless steel autoclave, and kept under an autogenous pressure at 160 °C for 72 h. After slow cooling to room temperature at a rate of 5 °C h^{-1}, red sheet crystals of **1** were manually isolated from colorless crystals (which proved to be $H_4SiW_{12}O_{40}$ by an IR spectra analysis), washed with distilled water, and air dried. Yield: 37.1 mg, 60% (based on pz). Anal. Calcd. for $C_{24}H_{24}N_{12}ClCu_5SiW_{12}O_{40}$(3707.92): C, 7.77; H, 0.65; N, 4.53; Si, 0.76; Cu, 8.57; W, 59.50 (%). Found: C, 7.82; H, 0.71; N, 4.43; Si, 0.69; Cu, 8.42; W, 59.31 (%). IR (KBr, cm^{-1}): ν 3452 (w), 3108 (w), 2900 (w), 1604 (w), 1483 (w), 1421 (m), 1158 (m), 1119 (w), 1061 (w), 1010 (m), 974 (m), 952 (m), 920 (s), 975 (m), 784 (s), 528 (m), 463 (m).

2.2.2. $[Ag_4(pz)_3(H_2O)_2(SiW_{12}O_{40})]$ (**2**)

The preparation of compound **2** was similar to that of **1**, except that an $AgNO_3$ (34 mg, 0.2 mmol) was used instead of $Cu(CH_3COO)_2\cdot 3H_2O$. Pale-yellow block crystals were isolated manually from a yellow powder (which was proved to be composed of Ag and pyrazine by an IR spectra analysis), washed with distilled water, and air dried. Yield: 65.6 mg, 55% (based on pz). Anal. Calcd. for $C_{12}H_{16}Ag_4N_6SiW_{12}O_{42}$(3582.08): C, 4.02; H, 0.45; N, 2.35; Si, 0.78; Ag, 12.04; W, 61.59 (%). Found: C, 3.91; H, 0.52; N, 2.41; Si, 0.71; Ag, 11.86; W, 61.42 (%). IR (KBr, cm^{-1}): ν 3604 (w), 3108 (w), 3039 (w), 1597 (w), 1485 (m), 1422 (s), 1150 (m), 1131 (m), 1079 (m), 1056 (m), 1011 (m), 970 (s), 918 (s), 878 (m), 788 (s), 535 (m), 444 (m).

2.3. X-ray crystallography

Suitable single crystals of compounds **1** and **2** were mounted on a Bruker-AXS CCD diffractometer equipped with a graphite-monochromated Mo $K\alpha$ radiation source (λ=0.07103 Å) at 298 K. The absorption corrections were performed with the SADABS program. The structures were solved by direct methods and expanded using Fourier techniques. The non-hydrogen atoms were refined anisotropically. Some hydrogen atoms were located in the calculated positions. All calculations were performed using the SHELXTL-97 program [45,46]. The crystallographic details of **1** and **2** are summarized in Table 1. The selected bond lengths and angles of **1** and **2** are listed in Tables S1 and S2, respectively.

3. Results and discussion

3.1. Synthesis

Compounds **1** and **2** were synthesized under almost the same hydrothermal conditions, except for using the different metal ions. The bond valence sum (BVS) calculations [47] of **1** resulted in an oxidation state in the range 1.118–1.243 (av. 1.172) for the copper centers, suggesting that all copper atoms in **1** are all in +1 oxidation state. The XPS spectra of **1** (Fig. S1) gives one peak at 932.85 eV, ascribed to $Cu^{+}2p_{3/2}$, further confirming the valence of Cu [48]. These results are consistent with the structure analysis. The main reason of the change for $Cu^{II}\rightarrow Cu^{I}$ is that pz acts as not only ligand, but also as reductant under the hydrothermal conditions. Such a phenomenon has been observed frequently in the hydrothermal reaction system containing N-donor ligands and Cu(II) ions [49]. All W atoms are in the +VI oxidation state, calculated by BVS calculations. So, the two compounds are formulated as $[Cu_5(pz)_6(Cl)(SiW_{12}O_{40})]$ (**1**) and $[Ag_4(pz)_3(H_2O)_2(SiW_{12}O_{40})]$ (**2**).

3.2. Structural description

The $SiW_{12}O_{40}^{4-}$ anion is the inorganic building block in compounds **1** and **2**. The W–O and Si–O bond distances are in the normal ranges [40,54]. The central atom Si in the two

Table 1
Crystal date and structure refinements for compounds **1** and **2**.

Compounds	**1**	**2**
Empirical formula	$C_{24}H_{24}ClCu_5N_{12}O_{40}SiW_{12}$	$C_{12}H_{16}Ag_4N_6O_{42}SiW_{12}$
M_r	3707.99	3582.08
Temperature (K)	293(2)	293(2)
Crystal system	Triclinic	Monoclinic
Space group	*P*-1	$P2_1/n$
a (Å)	11.7152(1)	12.7726(10)
b (Å)	13.5922(5)	14.4219(12)
c (Å)	20.6532(7)	12.8058(10)
α (deg.)	89.218(8)	90.00
β (deg.)	76.358(8)	100.272(5)
γ (deg.)	67.393(4)	90.00
V (Å^3)	2939.48(15)	2321.1(3)
Z	2	2
$D_{calc.}$ (g cm^{-3})	4.189	5.125
F(0 0 0)	3272	3104
Reflections collected/ unique	18,576/9844	16,665/5284
R_{int}	0.0963	0.0622
R_1[a]/wR_2[b][$I>2\sigma(I)$]	0.1072/0.2602	0.0927/0.2755
GOF on F^2	1.156	1.078

[a] $R_1=\Sigma||F_0|-|F_c||/\Sigma|F_0|=wR_2=\Sigma[w(F_0^2-F_c^2)^2]/\Sigma[w(F_0^2)^2]^{1/2}$.

compounds is disorderly surrounded by a cube of eight oxygen atoms, with each oxygen site half occupied. The structure feature of disorder often appears in the Keggin structure [24].

3.2.1. Structural of $[Cu_5(pz)_6(Cl)(SiW_{12}O_{40})]$ (**1**)

Crystal structure analysis reveals that the asymmetric unit of **1** contains two crystallographically independent half of $SiW_{12}O_{40}^{4-}$ (SiW_{12}) anion, hereafter labelled *A*-$[SiW_{12}O_{40}]^{4-}$ and *B*-$[SiW_{12}O_{40}]^{4-}$ in order to distinguish them, five Cu(I) ions, six pz ligands and one Cl anion. (Fig. 1).

In compound **1**, the Cu1 ion adopts the distorted tetrahedron geometry, coordinated by two N atoms from two pz ligands, one O atom from *A*-$[SiW_{12}O_{40}]^{4-}$ polyanion and one Cl anion, with Cu–N bond distances of 1.96(3) and 1.96(4) Å, Cu–O bond distance of 2.21(3) Å, Cu–Cl bond distance of 2.551(13), N–Cu–N angle of 132.0(15)°, and N–Cu–O angles of 99.5(14)° and 122.8(13)°. The Cu2 ion is three-coordinated in a trigonal geometry, coordinated by three N atoms from three pz ligands, with Cu–N bond distances of 1.95(3)–2.03(3) Å, N–Cu–N angles of 117.1(14)–122.4(14)°. The Cu3 ion adopts a distorted tetrahedron geometry, coordinated by three N atoms from three pz ligands and one Cl anion, with Cu–N bond distances of 2.02(3)–2.07(4) Å, Cu–Cl bond distance of 2.541(12) Å, and N–Cu–N angles of 115.3(14)–120.0(14)°. The Cu4 ion also adopts the distorted tetrahedron geometry, coordinated by three N atoms from three pz ligands and one O atom from the *B*-$[SiW_{12}O_{40}]^{4-}$ polyanion, with Cu–N bond distances of 1.96(4)–1.98(4) Å, Cu–O bond distance of 2.52(3) Å, and N–Cu–N angles of 105.0(15)–129.7(14)°. The Cu5 ion is four-coordinated in a "seesaw" geometry, coordinated by two O atoms from the *A*-$[SiW_{12}O_{40}]^{4-}$ polyanion, one N atoms from one pz ligand and one Cl anion, with Cu–N bond distances of 1.86(4) Å, Cu–O bond distance of 2.51(9) and 2.64(5) Å, Cu–Cl bond distance of 2.135(12) Å, N–Cu–O angle of 89.26(7)° and 90.5(0), and O–Cu–O angle of 119.6(8).

As shown in Fig. 2, the pz ligand and the Cl anion, acting as bridging linker, connect the adjacent Cu(I) ions to form a 6^3 topological 2-D cationic sheet with a 34-membered $Cu_8(pz)_6(Cl)_2$ ring *A* and a 30-membered $Cu_6(pz)_6$ ring *B*. The *A*-$[SiW_{12}O_{40}]^{4-}$ and *B*-$[SiW_{12}O_{40}]^{4-}$ polyanions are sandwiched between the adjacent sheets and coordinate with Cu(I) to form a "hamburger"-like layer unit, as shown in Fig. 3. Furthermore, the adjacent "hamburger"-like layers are linked by Cl bridges in ABAB fashion to construct a 3D framework (Fig. 4). From the topological view, the 3D structure can be rationalized as a (3,4)-connected network with $(6\cdot7\cdot8)(6^3\cdot7\cdot8^2)(6^3)(6^5\cdot7)(6^5\cdot8)$ topology, if we assign SiW_{12} clusters, pz ligands, and Cu5 atoms as the connectors and

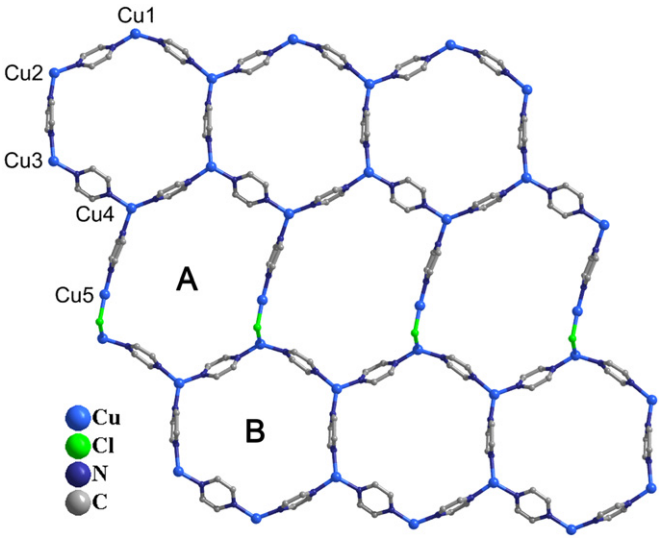

Fig. 2. The 2-D (6,3) topological net in **1** (H atoms are omitted for clarity).

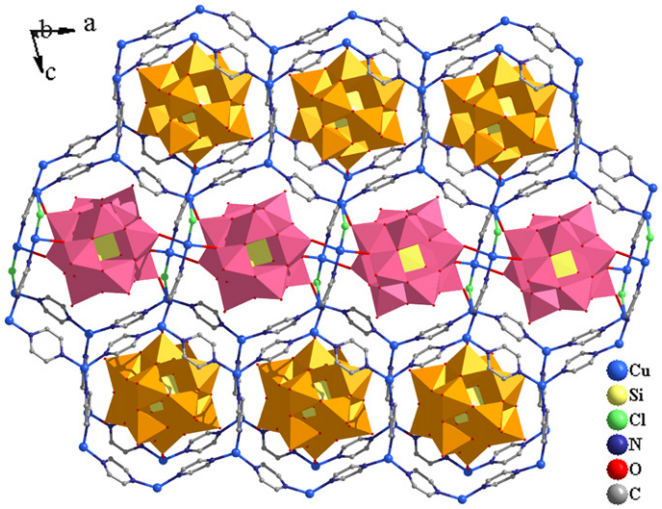

Fig. 3. Two adjacent cationic sheets sandwiching the *A*-$[SiW_{12}O_{40}]^{4-}$ (orange polyhedron) and *B*-$[SiW_{12}O_{40}]^{4-}$ (pick polyhedron) polyanions (H atoms are omitted for clarity).

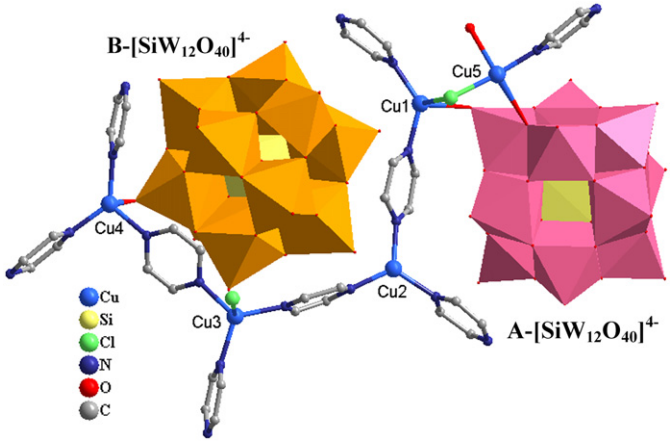

Fig. 1. Polyhedral and ball-and-stick representation of compound **1**. (H atoms are omitted for clarity).

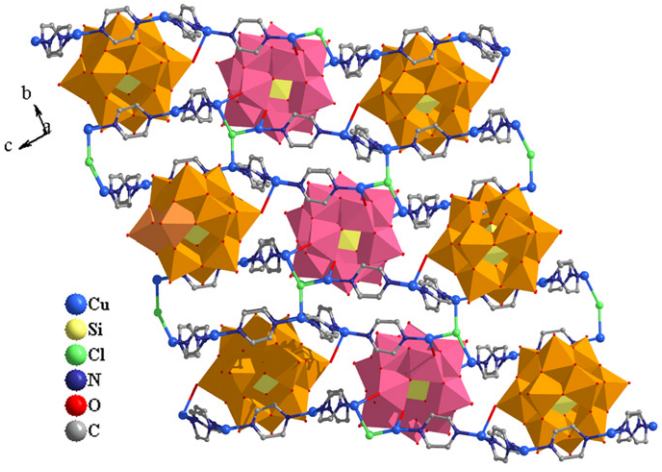

Fig. 4. View of the 3-D framework of **1** constructed from parallel "hamburger" layers connected by Cl ions along the *a* axis (H atoms are omitted for clarity).

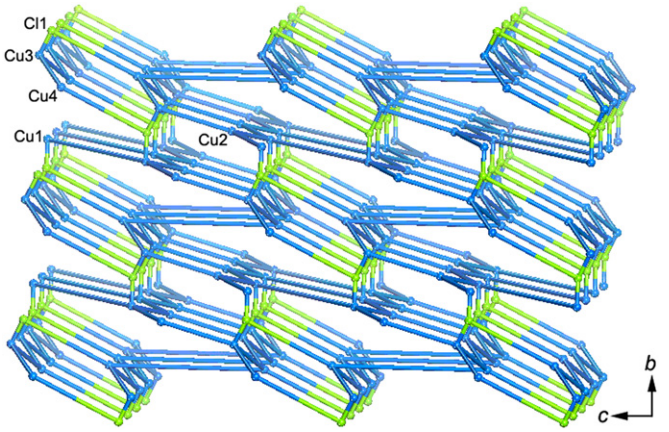

Fig. 5. Schematic view of the (3,4)-connected 5-nodal network with $(6\cdot7\cdot8)(6^3\cdot7\cdot8^2)(6^3)(6^5\cdot7)(6^5\cdot8)$ topology in **1** (blue balls represent Cu atoms, and green balls represent Cl atoms). (For interpretation of the references to color in this figure legend, the reader is referred to the web version of this article.)

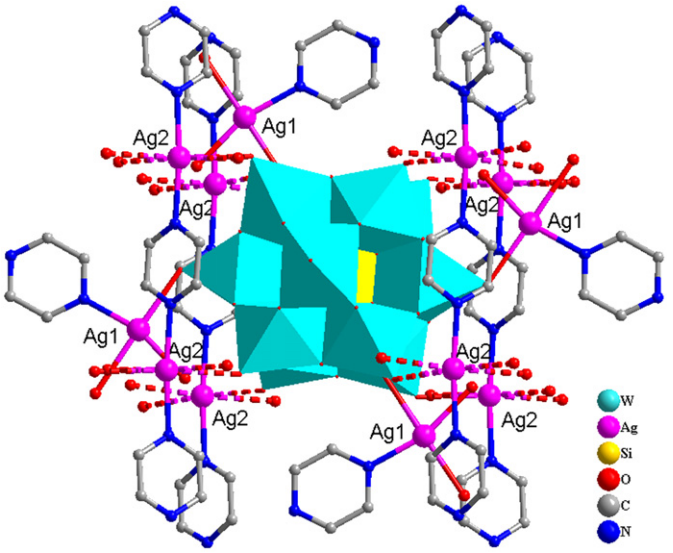

Fig. 6. Polyhedral and ball-and-stick representation of compound **2** (H atoms are omitted for clarity).

Cu1, Cu2, Cu3, Cu4, and Cl atoms as the nodes (Fig. 5). In this simplification, Cu2 and Cl atoms are the three-connected nodes, and Cu1, Cu3, and Cu4 atoms are the four-connected ones.

3.3. Structural of $[Ag_4(pz)_3(H_2O)_2(SiW_{12}O_{40})]$ (**2**).

Crystal structure analysis reveals that compound **2** consists of four Ag(I) ions, three pz ligands, one $SiW_{12}O_{40}^{4-}$ anion, and two H_2O molecules (Fig. 6).

In compound **2**, there are two crystallographically independent Ag ions. The Ag1 ion is four-coordinated in a square geometry, coordinated by one N atoms from one pz ligand and two O atoms from two different SiW_{12} anion and one aqua molecule. The bond distances and angles around Ag1 are 2.16(3) Å for Ag–N, 2.31(2) and 2.46(4) Å for Ag–O, 95.7(11)° and 163.0(1)° for N–Ag–O, and 101.2(10)° for O–Ag–O. The Ag2 ion is coordinated by two N atoms from two pz ligand with Ag–N bond distances of 2.24(3) and 2.25(3) Å and N–Ag–N angle of 174.2(10)°. It is noted that the Ag2 ion is surrounded by four O atoms from four different SiW_{12} anion and Ag–O distances of 2.72(6)–2.75(1) Å (the sum of the van der Waals radii of Ag and O is 3.2 Å) [50] imply the weak interaction. The coordination geometry around Ag2 is a rare distorted octahedron [51].

As shown in Fig. 7, each SiW_{12} anion acts as an inorganic tetradentata ligand covalently bonding to four Ag1 ions via two terminal and two bridging O atoms in the same plane. And two adjacent Ag1 ions are linked by the pz ligand. Thus, a $(5^3)_2(5^4\cdot8^2)$ topological 2-D net is generated, in which the SiW_{12} anion serves as a four-connected node, and Ag1 ion serve as a three-connected node. Furthermore, the adjacent layers are linked by the $[Ag2(pz)]_n^{n+}$ chains through Ag–O weak interactions to form a 3-D framework (Fig. 8). If these Ag–O non-covalent interactions are considered, each SiW_{12} anion can coordinate to twelve Ag(I) ions. From the topological view, if Ag1, Ag2, and SiW_{12} are viewed as three, six, and twelve connecting nodes, respectively, the structure of **2** can be symbolized as an intricate (3,6,12)-connected framework with $(3^4\cdot4^{16}\cdot5^{24}\cdot6^{12}\cdot7^8\cdot8^2)(3^4\cdot4^6\cdot5^4\cdot6)_2(4\cdot5^2)_2$ topology (Fig. 9). This represents the highest connected network topology presently known for polyoxometalate systems [29].

3.4. Influence of the metals on the structures of compounds **1** and **2**

Through the contrast between the two compounds, we think that the metal ions play the key role for the formation of the different structures. In compound **1**, the Cu(I) ions adopt three

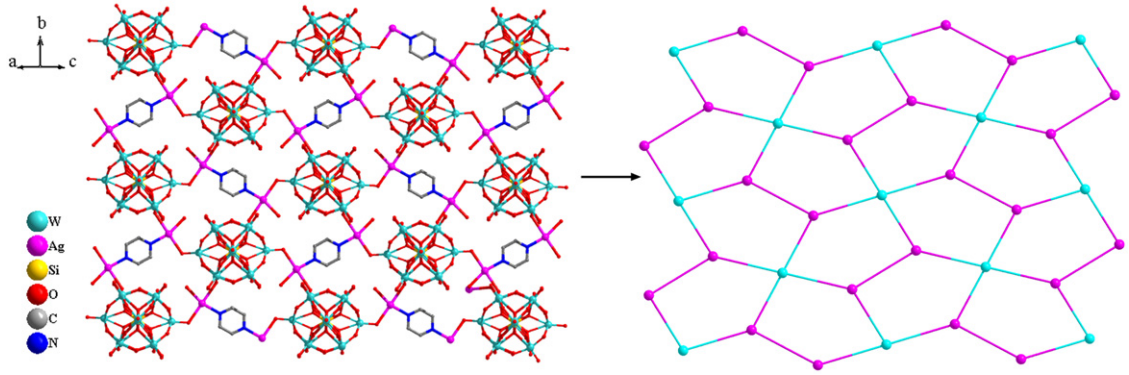

Fig. 7. . (left) View of the 2-D structure constructed by SiW_{12} anions and $Ag_2(pz)$ groups in **2** (H atoms are omitted for clarity). (right) Schematic view of the $(5^3)_2(5^4\cdot8^2)$ topology (blue balls represent SiW_{12} cluster, and pink ones represent Ag atoms). (For interpretation of the references to color in this figure legend, the reader is referred to the web version of this article.)

kinds of coordination geometries (tetrahedron, trigonal, and seesaw geometries), and link the pz ligands and Cl ions to construct a 6^3 topological 2-D sheet as a metal-organic unit. In compound **2**, the Ag(I) ions adopt two kinds of coordination geometries (square and octahedron geometries), and connect the pz ligands to form $Ag_2(pz)$ bridging groups and $[Ag(pz)]_n^{n+}$ chains. Furthermore, these differences induce different coordination behaviors of the SiW_{12} anions in the two compounds. In **1**, metal-organic sheets are connected covalently by SiW_{12} to form a sandwich double sheet. In **2**, the $Ag_2(pz)$ groups covalently connect the SiW_{12} anions to form a 2-D net, and the $[Ag(pz)]_n^{n+}$ chains linked the nets through non-covalent Ag–O interactions to extend to a 3D framework.

3.5. IR spectra

In the IR spectra of the two compounds (Fig. S2), the characteristic peaks at 1010, 974, 920, and 784 cm^{-1} for **1** and 1011, 970, 918, and 788 cm^{-1} for **2**, could be attributed to ν(Si–O_a), ν(W–O_d), ν(W–O_b–W), and ν(W–O_c–W) of the SiW_{12} polyanions, respectively, [52]. The peaks from 1100 to 1610 cm^{-1} could be regarded as the characteristics of the pz ligands.

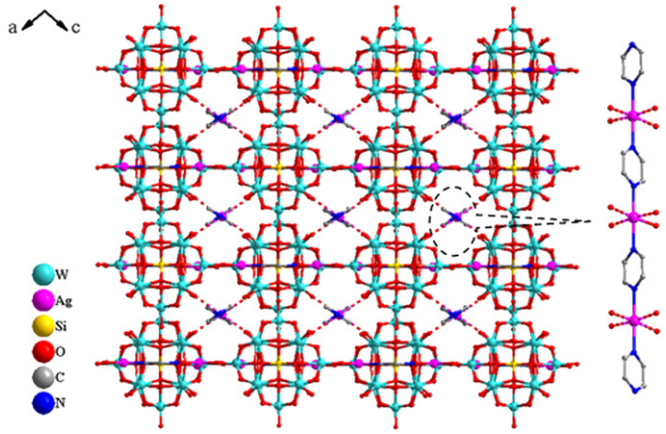

Fig. 8. View of the 3-D framework of **2** constructed from parallel layers linked by the $[Ag2(pz)]_n^{n+}$ chains along the *b* axis (H atoms are omitted for clarity).

3.6. Thermal analyses

Thermal gravimetric (TG) curves of compounds **1** and **2** are shown in Fig. S3. In compound **1**, the total weight loss of 12.01% (calc. 13.90%) from 235 to 410 °C is ascribed to decomposition of the pz ligands and Cl ions. At temperatures higher than 410 °C, compound **1** was slowly decomposed, which is considered as an oxidation reaction of carbon and reduction of W(VI), and carbon monoxide as an oxidation product was released [53]. The sample does not lose weight at temperatures higher than 720 °C. We speculate their final products of the thermal decomposition are the mixture of SiO_2, Cu_2O, and tungstous oxide, considering the nitrogen protected environment of the TG analyses procedure. For compound **2**, it shows a 0.97% weight loss between 160 and 230 °C, which corresponds to coordinated water (calc. 1.01%). The 6.41% weight loss (calcd. 6.71%) from 315 to 415 °C is ascribed to the release of the pz ligands. Higher than 700 °C, compound **2** does not lose weight, and their final products are SiO_2, Ag_2O and tungstous oxide.

3.7. Cyclic voltammetry

Redox properties of compounds **1** and **2** were studied in 1 M H_2SO_4 aqueous solution (Fig. 10). In the potential range +200 to −800 mV, three pairs of redox peaks (I–I', II–II', and III–III') are observed, with the peak potentials $E_{1/2}=(E_{pc}+E_{pa})/2$ at −238 (I–I'), −430 (II–II'), −618 (III–III') mV for compound **1** and $E_{1/2}=(E_{pc}+E_{pa})/2$ at −226 (I–I'), −432 (II–II'), −616 (III–III') mV for compound **2**, respectively. Thereinto, redox peaks I–I' and II–II' correspond to two consecutive one-electron processes of W atoms, while III–III' corresponds to a two-electron process [54–56]. The cyclic voltammetry measurements indicate that the two compounds keep the redox properties of their parent polyanions.

As shown in Fig. 11, **1**- and **2**-CPE display good electrocatalytic activity toward the reduction of nitrite in 1 M H_2SO_4 containing $NaNO_2$. For the **1**-CPE, with the addition of nitrite, all the three reduction peak currents increase markedly, while the corresponding oxidation peak currents decrease, suggesting that nitrite is reduced by the one-, two-, and four-electron reduced species of W atoms. Compared with the **1**-CPE, only the last two pairs of currents of 2-CPE were changed with the addition of nitrite, indicating that the nitrite is mainly reduced by the two- and four-electron reduced species of W atoms. The different

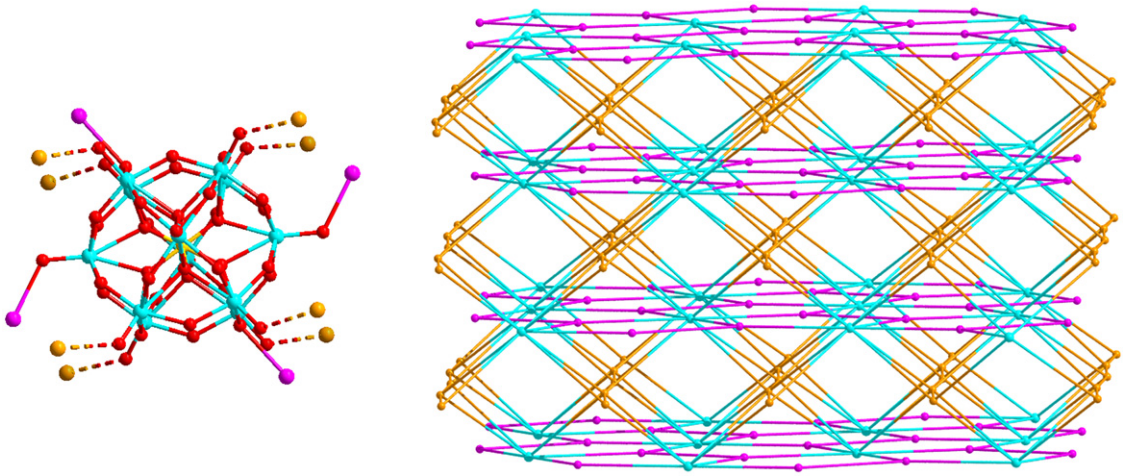

Fig. 9. . (left) The coordination mode of the SiW_{12} anion in **2** (the Ag–O interactions being considered). (right) Schematic view of the (3,6,12)-connected framework with $(3^4\cdot 4^{16}\cdot 5^{24}\cdot 6^{12}\cdot 7^8\cdot 8^2)(3^4\cdot 4^6\cdot 5^4\cdot 6)_2(4\cdot 5^2)_2$ topology in **2** (blue balls represent SiW_{12} clusters, pink balls represent Ag1 atoms, and orange balls represent Ag2 atoms). (For interpretation of the references to color in this figure legend, the reader is referred to the web version of this article.)

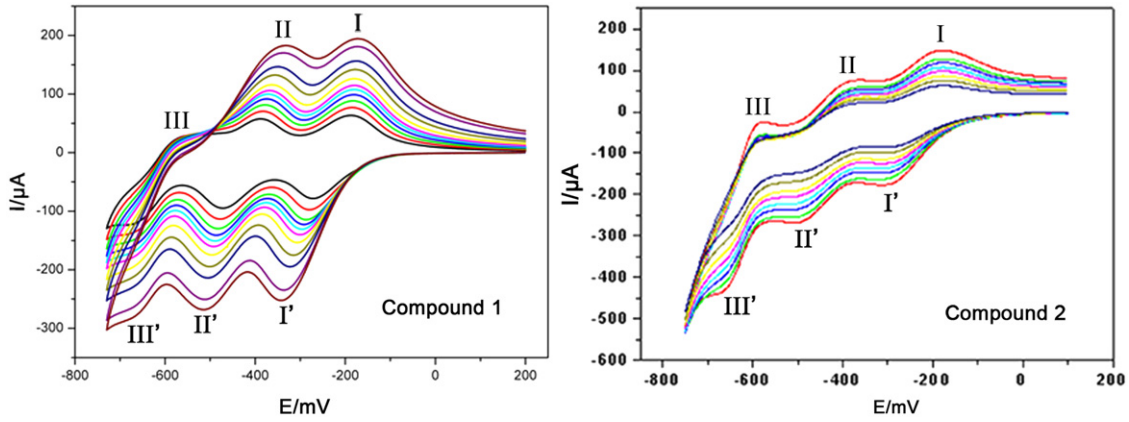

Fig. 10. The cyclic voltammograms of **1**- and **2**-CPEs in 1 M H_2SO_4 at the different scan rates. From inner to outer: for **1**-CPE, 60, 80, 100, 120, 140, 160, 200, 250, 300, 350, 400 mV s^{-1}; for **2**-CPE, 80, 100, 150, 200, 250, 300, 350, 400 mV s^{-1}.

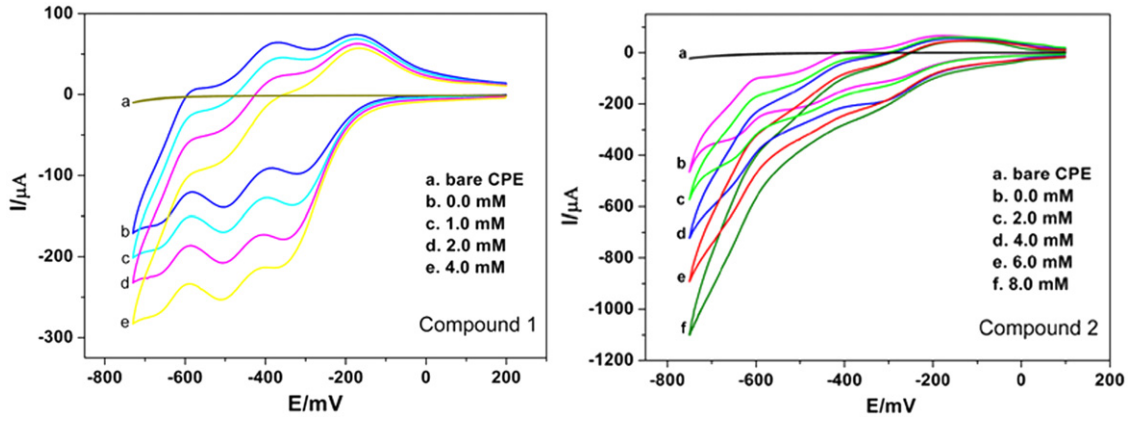

Fig. 11. Cyclic voltammograms of **1**-CPE and **2**-CPE in 1 M H_2SO_4 containing different concentrations of $NaNO_2$.

electrochemical behaviors of compounds **1** and **2** may be explainable, due to their different chemical environments [57].

4. Conclusions

In summary, two new inorganic–organic hybrid compounds based on Cu(I)/Ag(I), pyrazine, and Keggin polyanions have been successfully synthesized and structurally characterized. Their informative structures indicate that metal ions with different coordination numbers and geometries can form various metal-organic units, which also induce different coordination behaviors of the polyanions, and thus the final structures are influenced. In addition, the **1**- and **2**-CPE exhibit electrocatalytic activities towards the reduction of nitrite. Further investigation progress to provide more examples and information about the influence of other metal ions on the structures of POM-based compounds.

Acknowledgments

This work was supported by the Natural Science Fund Council of China (NSFC, Nos. 10876002, 20731002, 20701011, 20801005, 20801004), Doctoral Program of Higher Education (SRFDP, No. 200800070015), Open Fund of State Key Laboratory of Explosion Science and Technology, Beijing Institute of Technology (No. ZDKT08-01), the 111 Project B07012 in China, and the Key Project of Chinese Ministry of Education (No. 208116).

Appendix A. Supplementary material

Supplementary data associated with this article can be found in the online version at doi:10.1016/j.jssc.2010.09.034.

References

[1] N.K. Al-Rasbi, I.S. Tidmarsh, S.P. Argent, H. Adams, L.P. Harding, M.D. Ward, J. Am. Chem. Soc. 130 (2008) 11641.
[2] D.J. Tranchemontagne, Z. Ni, M. O'Keeffe, O.M. Yaghi, Angew. Chem. Int. Ed. 47 (2008) 5136.
[3] T.K. Ronson, J. Fisher, L.P. Harding, M.J. Hardie, Angew. Chem. Int. Ed. 46 (2007) 9086.
[4] S. Kitagawa, R. Kitaura, S.I. Noro, Angew. Chem. Int. Ed. 43 (2004) 2334.
[5] E.A. Nytko, J.S. Helton, P. Müller, D.G. Nocera, J. Am. Chem. Soc. 130 (2008) 2922.
[6] M. Fujita, Y.J. Kwon, S. Washizu, K. Ogura, J. Am. Chem. Soc. 116 (1994) 1151.
[7] M.T. Pope, A. Müller, in: Polyoxometalate Chemistry: from Topology via Self-assembly to Applications, Kluwer, Dordrecht, The Netherlands, 2001.
[8] J.J. Borrys-Almener, E. Coronado, A. Müller, M.T. Pope, in: Polyoxometalate Molecular Science, Kluwer, Dordrecht, The Netherlands, 2003.
[9] D.L. Long, E. Burkholder, L. Cronin, Chem. Soc. Rev. 36 (2007) 105.
[10] N. Mizuno, M. Misono, Chem. Rev. 98 (1998) 199.
[11] A. Müller, C. Serain, Acc. Chem. Res. 33 (2000) 2.
[12] C.L. Hill, Chem. Rev. 98 (1998) 1.
[13] T. Yamase, Chem. Rev. 98 (1998) 307.
[14] C.Y. Duan, M.L. Wei, D. Guo, C. He, Q.J. Meng, J. Am. Chem. Soc. 132 (2010) 3321.
[15] L.M. Rodriguez-Albelo, A.R. Ruiz-Salvador, A. Sampieri, et al., J. Am. Chem. Soc. 131 (2009) 16078.
[16] S.-T. Zheng, J. Zhang, G.-Y. Yang, Angew. Chem. Int. Ed. 47 (2008) 3909.
[17] A. Yokoyama, T. Kojima, K. Ohkubo, S. Fukuzumi, Chem. Commun. (2007) 3997.

[18] C. Streb, C. Ritchie, D.-L. Long, P. Kögerler, L. Cronin, Angew. Chem. Int. Ed. 46 (2007) 7579.
[19] Y.-F. Song, D.-L. Long, L. Cronin, Angew. Chem. Int. Ed. 46 (2007) 3900.
[20] C.-Y. Sun, S.-X. Liu, D.-L. Liang, K.-Z. Shao, Y.-H. Ren, Z.-M. Su, J. Am. Chem. Soc. 131 (2009) 1883.
[21] X.L. Wang, C. Qin, E.B. Wang, Z.M. Su, Y.G. Li, L. Xu, Angew. Chem. Int. Ed. 45 (2006) 7411.
[22] A. Dolbecq, C. Mellot-Draznieks, P. Mialane, J. Marrot, G. Férey, F. Sécheresse, Eur. J. Inorg. Chem. (2005) 3009.
[23] X.L. Wang, Y.F. Bi, B.K. Chen, H.Y. Lin, G.C. Liu, Inorg. Chem. 47 (2008) 2442.
[24] C.-H. Li, K.-L. Huang, Y.-N. Chi, X. Liu, Z.-G. Han, L. Shen, C.-W. Hu, Inorg. Chem. 48 (2009) 2010.
[25] E. Burkholder, V. Golub, J.C. O'Connorr, J. Zubieta, Inorg. Chem. 43 (2004) 7014.
[26] R.S. Rarig, J. Zubieta, J. Chem. Soc., Dalton Trans. (2001) 3446.
[27] Z.Y. Shi, J. Peng, C.J. Gómez-García, S. Benmansour, X.J. Gu, J. Solid State Chem. 179 (2006) 253.
[28] B.-X. Dong, J. Peng, C.J. Gómez-García, S. Benmansour, H.-Q. Jia, N.-H. Hu, Inorg. Chem. 46 (2007) 5933.
[29] Y.-Q. Lan, S.-L. Li, K.-Z. Shao, X.-L. Wang, Z.-M. Su, Dalton Trans. (2008) 3824.
[30] A.-X. Tian, J. Ying, J. Peng, J.-Q. Sha, Z.-G. Han, J.-F. Ma, Z.-M. Su, N.-H. Hu, H.-Q. Jia, Inorg. Chem. 47 (2008) 3274.
[31] A.-X. Tian, J. Ying, J. Peng, J.-Q. Sha, Z.-M. Su, H.-J. Pang, P.-P. Zhang, Y. Chen, M. Zhu, Y. Shen, Cryst. Growth Des. 10 (2010) 1104.
[32] A.-X. Tian, J. Ying, J. Peng, J.-Q. Sha, H.-J. Pang, P.-P. Zhang, Y. Chen, M. Zhu, Z.-M. Su, Cryst. Growth Des. 8 (2008) 3717.
[33] P.J. Hagrman, R.L. LaDuca, H.J. Koo, R. Rarig, R.C. Haushalter, M.H. Whangbo, J. Zubieta, Inorg. Chem. 39 (2000) 4311.
[34] Y.-P. Ren, X.-J. Kong, J.L.-S. Long, R.-B. Huang, L.-S. Zheng, Cryst. Growth Des. 6 (2006) 572.
[35] J.-Q. Sha, J. Peng, A.-X. Tian, H.-S. Liu, J. Chen, P.-P. Zhang, Cryst. Growth Des. 7 (2007) 2535.
[36] J.-Q. Sha, J. Peng, Y. Zhang, H.-J. Pang, A.-X. Tian, P.-P. Zhang, H. Liu, Cryst. Growth Des. 9 (2009) 1708.
[37] P.-Q. Zheng, Y.-P. Ren, L.-S. Long, R.-B. Huang, L.-S. Zheng, Inorg. Chem. 44 (2005) 1190.
[38] J.-Q. Sha, J. Peng, Y.Q. Lan, Z.M. Su, H.J. Pang, A.X. Tian, P.P. Zhang, M. Zhu, Inorg. Chem. 47 (2008) 5145.
[39] H.X. Yang, S.Y. Gao, J. Lu, B. Xu, J.X. Lin, R. Cao, Inorg. Chem. 49 (2010) 736.
[40] S.-L. Li, Y.-Q. Lan, J.-F. Ma, J. Yang, J. Liu, Y.-M. Fu, Z.-M. Su, Dalton Trans. (2008) 2015.
[41] Y.-Q. Lan, S.-L. Li, X.-L. Wang, K.-Z. Shao, D.-Y. Du, H.-Y. Z, Z.-M. Su, Inorg. Chem. 47 (2008) 8179.
[42] Y.-P. Ren, X.-J. Kong, X.-Y. Hu, M. Sun, L.-S. Long, R.-B. Huang, L.-S. Zheng, Inorg. Chem. 45 (2006) 4016.
[43] P.-Q. Zheng, Y.-P. Ren, L.-S. Long, R.-B. Huang, L.-S. Zheng, Inorg. Chem. 44 (2005) 1190.
[44] Y.-P. Ren, X.-J. Kong, J.L.-S. Long, R.-B. Huang, L.-S. Zheng, Cryst. Growth Des. 6 (2006) 572.
[45] G.M. Sheldrick, 1997. SHELXS 97, Program for Crystal Structure Solution, University of Göttingen, Göttingen, Germany.
[46] G. M. Sheldrick, 1997. SHELXL 97, Program for Crystal Structure Refinement, University of Göttingen, Göttingen, Germany.
[47] I.D. Brown, D. Altermatt, Acta Crystallogr. Sect. B (1985) 4124.
[48] Y.-H. Liu, G.-L. Guo, J.-P. Wang, J. Coord. Chem. 61 (2008) 2428.
[49] Y.-N. Chi, F.-Y. Cui, Y.-Q. Xu, C.-W. Hu, Eur. J. Inorg. Chem. (2007) 4375.
[50] A. Bondi, J. Phys. Chem. 68 (1964) 441.
[51] Z.G. Han, Y.Z. Gao, C.W. Hu, Cryst. Growth Des. 8 (2008) 1261.
[52] R. Thouvenot, M. Fournier, R. Franck, G. Rocchiccioli-Deltche, Inorg. Chem. 23 (1984) 598.
[53] S. Liu, Y.-G. Chen, D.-M. Shi, H.-J. Pang, Inorg. Chim. Acta 361 (2008) 2343.
[54] M. Sadakane, E. Steckhan, Chem. Rev. 98 (1998) 219.
[55] A.X. Tian, J. Ying, J. Peng, J.Q. Sha, H.J. Pang, P.P. Zhang, Y. Chen, M. Zhu, Z.M. Su, Inorg. Chem. 48 (2009) 100.
[56] J. Liu, Y.G. Li, E.B. Wang, D.R. Xiao, L.L. Fan, Z.M. Zhang, Y. Wang, J. Mol. Struct. 837 (2007) 237.
[57] J.Q. Sha, J. Peng, H.S. Liu, J. Chen, A.X. Tian, P.P. Zhang, Inorg. Chem. 46 (2007) 11183.